

Article

Implications of Bioenergy Cropping for Soil: Remote Sensing Identification of Silage Maize Cultivation and Risk Assessment Concerning Soil Erosion and Compaction

Thorsten Ruf ^{1,*} , Mario Gilcher ², Thomas Udelhoven ² and Christoph Emmerling ¹

¹ Department of Soil Science, Faculty of Regional and Environmental Sciences, University of Trier, 54296 Trier, Germany; emmerling@uni-trier.de

² Department of Environmental Remote Sensing and Geoinformatics, Faculty of Regional and Environmental Sciences, University of Trier, 54296 Trier, Germany; gilcher@uni-trier.de (M.G.); udelhoven@uni-trier.de (T.U.)

* Correspondence: ruf@uni-trier.de; Tel.: +49-651-201-3581

Abstract: Energy transition strategies in Germany have led to an expansion of energy crop cultivation in landscape, with silage maize as most valuable feedstock. The changes in the traditional cropping systems, with increasing shares of maize, raised concerns about the sustainability of agricultural feedstock production regarding threats to soil health. However, spatially explicit data about silage maize cultivation are missing; thus, implications for soil cannot be estimated in a precise way. With this study, we firstly aimed to track the fields cultivated with maize based on remote sensing data. Secondly, available soil data were target-specifically processed to determine the site-specific vulnerability of the soils for erosion and compaction. The generated, spatially-explicit data served as basis for a differentiated analysis of the development of the agricultural biogas sector, associated maize cultivation and its implications for soil health. In the study area, located in a low mountain range region in Western Germany, the number and capacity of biogas producing units increased by 25 installations and 10,163 kW from 2009 to 2016. The remote sensing-based classification approach showed that the maize cultivation area was expanded by 16% from 7305 to 8447 hectares. Thus, maize cultivation accounted for about 20% of the arable land use; however, with distinct local differences. Significant shares of about 30% of the maize cultivation was done on fields that show at least high potentials for soil erosion exceeding 25 t soil ha⁻¹ a⁻¹. Furthermore, about 10% of the maize cultivation was done on fields that pedogenetically show an elevated risk for soil compaction. In order to reach more sustainable cultivation systems of feedstock for anaerobic digestion, changes in cultivated crops and management strategies are urgently required, particularly against first signs of climate change. The presented approach can regionally be modified in order to develop site-adapted, sustainable bioenergy cropping systems.



Citation: Ruf, T.; Gilcher, M.; Udelhoven, T.; Emmerling, C. Implications of Bioenergy Cropping for Soil: Remote Sensing Identification of Silage Maize Cultivation and Risk Assessment Concerning Soil Erosion and Compaction. *Land* **2021**, *10*, 128. <https://doi.org/10.3390/land10020128>

Received: 20 December 2020

Accepted: 27 January 2021

Published: 29 January 2021

Publisher's Note: MDPI stays neutral with regard to jurisdictional claims in published maps and institutional affiliations.



Copyright: © 2021 by the authors. Licensee MDPI, Basel, Switzerland. This article is an open access article distributed under the terms and conditions of the Creative Commons Attribution (CC BY) license (<https://creativecommons.org/licenses/by/4.0/>).

Keywords: biomethantion; biogas; environmental impact; land use; risk assessment; soil management strategy

1. Introduction

The cultivation of energy crops on arable land aiming to substitute fossil fuels has significantly increased during the past decade [1]. In the course of Germany's energy transition strategy, numerous farmers have taken the opportunity to integrate agricultural energy production as a second mainstay with long-term governmentally guaranteed feed-in-tariffs [2,3].

Since silage maize was identified to be the most economically important crop for anaerobic digestion under temperate conditions, the cultivation area for energy crops has been significantly expanded; in Germany for example, from 200,000 to more than 900,000 hectares (ha) in the last decade [4–8]. However, introducing energy crops as a substrate for anaerobic digestion has implied changes in the traditional, cereal, and

grassland dominated agricultural system. As a consequence, the share of silage maize in crop rotations has increased and it is being cultivated on arable land, which has formerly never been used for the growing of row crops.

In the course of rising awareness about negative externalities associated with energy crop cultivation, the sustainability of silage maize cultivation has become a lively debate. Aspects, such as depletion of soil organic matter, which would certainly counteract the carbon dioxide saving targets, loss of agrobiodiversity, and the increased vulnerability of maize stands to soil erosion and compaction, are currently discussed, mainly based on statistical data about expanded silage maize cultivation [9–12]. However, using statistical data referring to large-scale areas like national territories or federal states to describe changes in the agricultural system and to evaluate consequences for the environment is hardly helpful and largely ignores contributing factors governed by site-specific conditions. For example, the erosion potential depends on the cultivated crop and specific management operations like tillage intensity but also on the terrain inclination, texture-governed soil erodibility, slope length, and erosivity of rainfall. Thus, a fact-based debate about hazards and implications of silage maize cultivation necessarily requires spatially-explicit data of the cultivated areas and additional information, including soil and climatic data, as well as structural parameters of the landscape and the agroecosystem. Simultaneously, such an approach requires to be conducted on a scale that allows matching spatially heterogeneity of environmental factors.

The present study aimed to reach conclusions on the implications of expanded silage maize cultivation for soil threats, particularly erosion and compaction in a low mountainous agricultural region. However, spatially-explicit census data were not available. Thus, firstly, a model application for detecting maize cultivation using RapidEye satellite images (Planet Labs Inc., San Francisco, CA, USA) was established for the years 2009 and 2016. We hypothesized that the established remote sensing-based classification approach allows tracking changes in the maize cultivation area with progressing expansion of agricultural biogas producing units (BPU). Therefore, additional data sources like statistical data and registers about BPUs were systematically screened. Secondly, a target-specific analysis of existing soil data was conducted to (i) identify pedotopes that are susceptible for soil compaction during harvest of silage maize in late autumn and (ii) to model the susceptibility of the soils for erosion by water (hereinafter referred to as 'erosion'). In order to achieve the overarching goal of this study, the results of the maize classification and the evaluation of the hazard potential caused by maize cultivation on the soil resource were combined. We hypothesized that the increased demand of feedstocks for anaerobic digestion led to pressure on soil resources and an expansion of the maize cultivation on sites that appear not suitable in a sustainable manner.

2. Materials and Methods

2.1. Characterization of the Study Area

The study was conducted in the administrative district 'Eifelkreis Bitburg-Prüm' (in the following referred to as 'study area'), which is located in the Federal State of Rhineland-Palatinate in the southwestern part of Germany. The rural nature of the study area is underlined by a population density of 59.8 inhabitants km⁻² and the dominance of agricultural land use, which accounts for 53.2% of the total area [13]. The study area was selected because statistical data indicate an intense development of the biogas sector from two BPUs in the year 2000 to 62 BPUs in the year 2016; associated with a distinct increase in silage maize cultivation (Figure 1) [14–16].

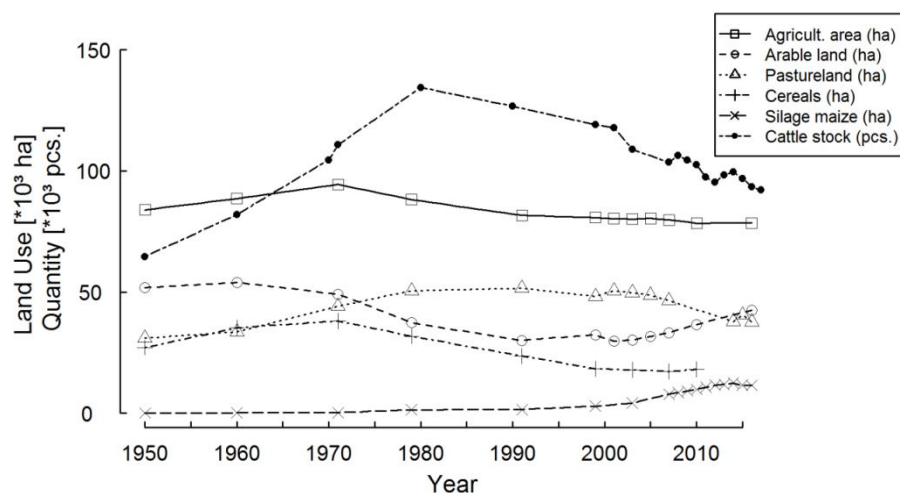


Figure 1. Development of the land-use (cereals excluding silage maize) and of the agricultural structure in the study region during the last decades based on census data [14,15].

The study area has a size of 1626 km² and spans an inclined plateau; the elevation climbs from 300 to 550 m a.s.l. in a south–north direction and peaks in the northern parts with hills of nearly 700 m a.s.l. The plateau is pervaded by numerous deep valley incisions with the main flow direction to the south. This pattern leads to a wavy, tightly structured landscape [17,18].

As a result of the elevation profile, the climatic conditions in the study area show a large latitudinal gradient (see Supplementary Material Table S1). Its southernmost parts are influenced by the viticultural climate of the Moselle valley with mild winters (mean annual temperature (MAT): 9.0 °C; mean annual precipitation (MAP): 861 mm a^{−1}), whereas the northern part shows a harsh low mountain range climate with distinctly lower MAT, as well as cold and long-lasting, precipitation-rich winters (MAT: 7.0 °C; MAP: 1250 mm a^{−1}) [19]. This general pattern is disrupted by the deep valleys which are characterized by considerably milder winters and warmer summers.

In the northern part of the study area, Devonian rocks are dominating whereas in the southern part, a small-scale co-existence of Triassic and Jurassic rocks can be found which are moreover partially overlaid by varying amounts of Quaternary sediments (loess) [20]. From these parent materials, in the northern part of the study area, silty to clayey Regosols and Cambisols developed. Soils that developed from Lower Triassic sediment rocks in the central and eastern part of the study area can be classified as sandy and clayey Regosols and Cambisols with alternating levels of loess. The small scale variability of parent materials in the southern part results in a mosaic of soils; the textures are mainly silt-loam, occasionally sandy and clayey. A wide range of soil types are present: Regosols, Cambisols, Stagnosols, Luvisols, and Vertisols whereby the both last mentioned soil types frequently tend to show signs of stagnant water [20–22].

Due to the gradient in climatic conditions and soils, the agricultural land in the northern part of the study area was traditionally dominated by grassland use whereas the more southern parts were characterized by cereal-based crop cultivation. Grain maize is not cultivated in the study area.

2.2. Remote Sensing Based Classification of Maize Fields

Farmers themselves, as well as governmental bodies, generally track crop types for cultivated areas very thoroughly. This kind of data is, unfortunately, rarely available to the public, nor to researchers, mostly because of privacy issues. Surveying the crop types manually by going out to the field or by asking farmers to access their records leads to a sparse or heavily spatially biased set of reference data. In order to have spatial explicit data about silage maize cultivation at hand, a remote sensing-based classification was conducted.

2.2.1. Selection and Pre-Processing of Remote Sensing Data

The classification approach was designed for a binary classification of maize and non-maize cultivation. The availability of suitable, gap-free coverages of the entire study area was of vital importance. The acquisition window was limited by the phenologic cycle of maize, which reaches the peak vegetation cover around the end of August. Using earlier imagery would result in emerging maize fields that show large soil fractions, while after August, there is the potential of early harvests. The third major constraint was the availability of high-resolution aerial photos on GoogleEarth, since these were used to produce reference data. After reviewing all available products, two RapidEye scenes in 2009 and 2016 met all three requirements. These two scenes were then atmospherically corrected based on the 5S algorithm [23] using the software AtCPro [24,25] and mosaicked together to one single image per year. A flowchart showing the steps of data processing and modeling is presented as Supplementary Material Figure S1.

2.2.2. Preparation of Reference Data

Since the classification of around 87,000 hectares of agricultural land requires a large amount of uniformly distributed training data, a visual survey approach was pursued. Based on GoogleEarth aerial imagery, it was trivial to distinguish maize fields from other agricultural crops, mostly cereals, and grassland. This is because maize is a high-growing row crop and has thus a very apparent texture which facilitates visual object recognition.

To guarantee an even distribution of training fields across the study area, it was split in subdivisions with 9 by 12 grids, with each cell spanning 5 by 5 km (Figure 2). The main goal was to select a representative set of training fields with at least three polygons, each with and without maize in every grid. Overall 2566 polygons were digitized for both years combined, amounting to almost 2000 hectares of maize fields per year. This represents about 20% of the overall acreage; the grid-cell approach in selecting training field should guarantee that the selected pixels are representative for the entire study area.

2.2.3. Pixel-Based Classification of Imagery

The classifications of all, roughly, 35,000,000 RapidEye pixels was done individually for both years using the random forest implementation of the ranger package in R programming language version 3.3.2 [26,27]. The random forest approach is a classifier that is based on the votes of randomly generated decision trees [28]. This particular approach was chosen because it scales well with a high number of features, as well as observations [27]. Furthermore, it is widely used for pixel-based land cover classification, because of its high accuracy and insensitivity to overfitting [29]. The classifications of both years trained with relatively high out-of-bag Cohens kappa values (index derived from expected agreement by chance, and observed agreement of classification with ground truth), but the classifier showed a slightly weaker performance in 2016 (Table 1). The high sensitivity values (true positive rate: quotient of pixels correctly classified as maize and pixels that are truly maize) mean that essentially all digitized maize fields were identified. The comparatively low specificity (true negative rate: quotient of pixels correctly classified as nonmaize and pixels that are truly nonmaize) indicates that there were a lot of false positives, meaning pixels that were classified as maize, but digitized as non-maize. After the classification with ranger, the probabilities were smoothed with a Gaussian kernel (see also Supplementary Material Figure S1). In a nutshell, the Gaussian kernel is a probability function. In the process of classifying a certain pixel, it takes into account the classification of the surrounding pixels in order to reduce the amount of noise in the prediction.

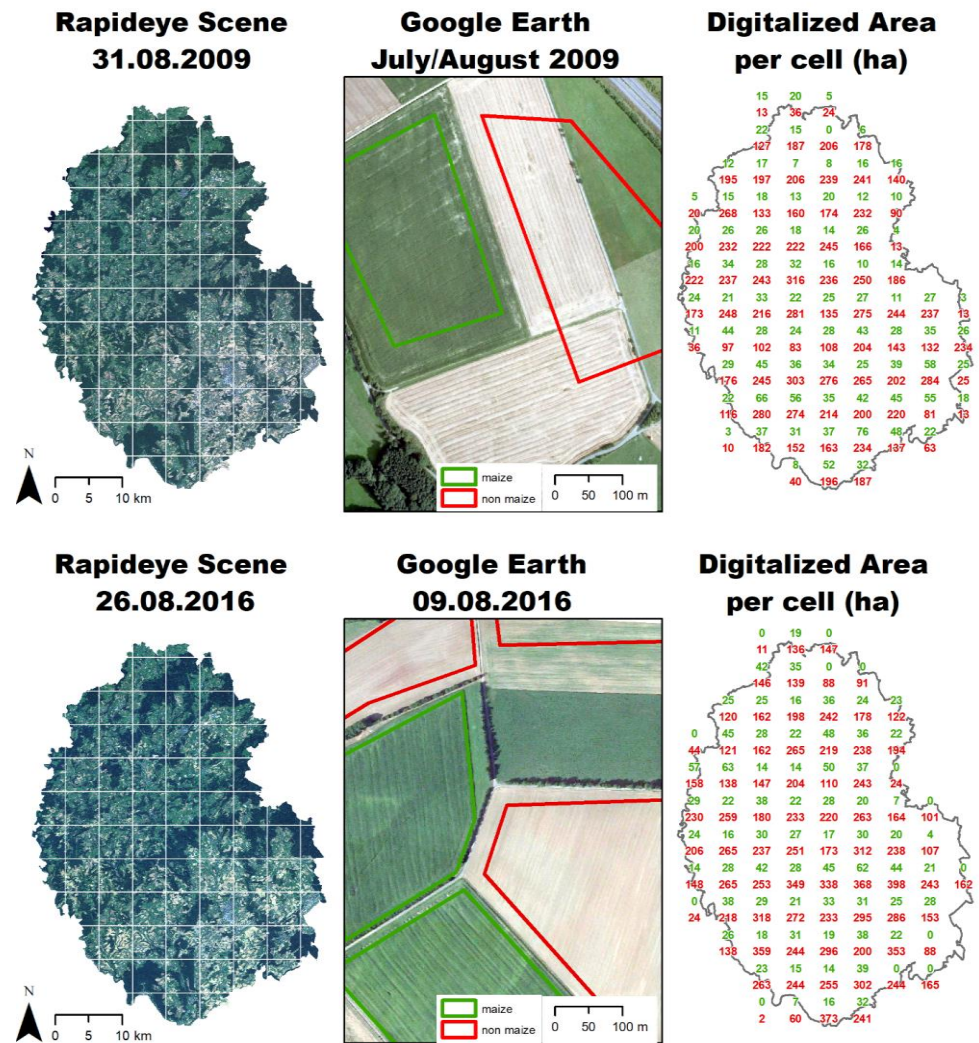


Figure 2. RapidEye coverage of the study area and manual digitization of reference data for the years 2009 (top) and 2016 (bottom).

Table 1. Summary of parameters specifying the efficiency of the selected approach for classification of maize fields.

Year	Sensitivity	Specificity	Kappa
2009	>0.99	~0.97	~0.97
2016	>0.99	~0.91	~0.93

2.3. Agricultural Biogas Producing Units

As defined in our hypotheses, we assumed that agricultural biogas plants are the main drivers for expanded silage maize cultivation. To be able to relate silage maize cultivation and feedstock demands, the locations of all agricultural BPUs, as well as their installed capacities in the course of time, were compiled based on (i) administrative data, (ii) ‘grey’ directories, and (iii) surveys of plant operators from third parties for internal use (references cannot be stated due to confidentiality agreement) due to the fact that no dataset was complete and up-to date, and contradictory data existed. The installed capacities of combined heat and power units located at remote places to supply local demands were ascribed to the digestion units since the demand for substrates is given there.

2.4. Determining of Pedotopes Susceptible for Compaction during Maize Harvesting

Soils that are particularly susceptible for soil compaction, with respect to maize harvesting operations in late autumn typically belong to the classes of Stagnosols and Planosols. These soils show horizons with very low permeability for water in the subsoil ('Sd' or 'Bg' horizon, acc. to [30] and [31], respectively) and tend to show waterlogging resulting from abundant autumn precipitation and low evaporation rates. Thus, in the period of silage maize harvesting, i.e., in late autumn, Stagnosols and Planosols frequently show high soil water contents resulting in low mechanical carrying capacities. These circumstances commonly result in serious soil compaction and structural damages caused by the heavy equipment used for silage maize harvesting.

For the purpose of this study, we performed a risk assessment for the soils concerning their vulnerability for soil compaction. Classification of soil types was based on the site specific sequence of soil horizons recorded in the framework of German land appraisal, which still represents the data basis for soils with the highest resolution and coverage (national law on farm land appraisal: [32]). The size of soil units in this framework is about one hectare. The sequence of the soil horizons was compared to a self-developed, predefined classification key using RStudio programming language version 3.3.2 [26]. In case that the sequence of soil horizons was in compliance with the key, a soil type was classified. Sequences of soil horizons that were not listed in the key were, as far as they were interpretable and meaningful, manually added to the key in iterative steps (flowchart of the classification presented as Supplementary Material Figure S2). However, data were only available for 55.3% of the agricultural area and for 36.3% the data basis was sufficient for soil type classification. For further analysis, soil types were grouped according to their specific vulnerability for soil compaction during harvesting operations of silage maize in late autumn as shown in Table 2.

Table 2. Classification of soil types regarding their susceptibility for soil compaction during harvesting operations of silage maize.

Susceptibility for Soil Compaction	Soil Types
High	Stagnosols, Planosols
Medium	<ul style="list-style-type: none"> • Transition soil types that show stagnic or gleyic properties but are not assigned to the class of Stagnosols or Planosols such as e.g., stagnic Cambisols, stagnic Fluvisol or stagnic Anthrosols. • Soils that are influenced by groundwater like Gleysols
Low	All other soil types

2.5. Determining of Site-Specific Susceptibility for Soil Erosion by Water

Natural proneness of the agricultural sites for soil erosion (E_{nat}) was modeled on pixel basis (grid resolution: 5 m \times 5 m) according to [33], using a simplified version of the universal soil loss equation (USLE) [34]. Modeling was done using ESRI's ArcMap 10.5. Input variables were:

- Slope factor (S): Slopes were calculated based on a digital elevation model with a resolution of 5 m (DEM5) provided by the [17]. The slope allowed calculating the slope factor using equation 7 given in [33].
- Soil erodibility factor (K): Derived from the soil texture of the topsoil determined in the framework of the German land appraisal. Textures were then assigned to K factors and corrected by soil skeleton and organic carbon contents using Equations (3)–(6), given in [33]. Values of the K factor for the study area with a raster resolution of 5 m by 5 m were provided by the State Office for Geology and Mining Rhineland Palatinate.
- Rainfall and runoff factor (R): R factors were calculated using the following regression equation: $R = 0.0788 * \text{mean annual precipitation (in mm)} * -2.82$ which was valid for the Federal Republic of Germany. Values of the R factor for the study area with a

raster resolution of 1 km by 1 km were provided by the State Office for Geology and Mining Rhineland Palatinate.

S, K, and R factors were multiplied for each raster cell. E_{nat} values were classified using the scheme presented in Table 3. Compared to the [33], the classes of erosion potential were considerably enlarged in order to take into account the fact that the study region is located in a low mountain region (consider also Figure 7).

Table 3. Assignment of calculated soil losses (E_{nat}) to classes of erosion potential.

Soil Erosion Potential	Soil Loss acc. to E_{nat} $t\ ha^{-1}\ a^{-1}$
Very low	<5
Low	5–10
Medium	10–25
High	25–50
Very high	>50

2.6. Data Analysis and Mapping

The analysis of data was done using RStudio programming language version 3.3.2 [26] and ArcMap 10.5 (ESRI Inc.). Maps were created using ArcMap 10.2.

3. Results and Discussions

3.1. Maize Classification

The classification approach to detect silage maize cropping sites has estimated a cultivation area of 7305 ha in 2009 and 8447 ha in 2016. In contrast to that, the official statistical records state values of 9147 ha and 11,496 ha in 2009 and 2016, respectively [15]. This means that the classifier underestimated the total maize cultivation area by roughly 2000 (2009) and 3000 ha (2016) compared to the official statistics (Table 4).

Table 4. Results of the silage maize classification approach using remote-sensing data compared to statistical data.

Year	Remote-Sensing Based Approach	Statistical Data	Difference between stat. Data and Remote-Sensing Based Approach	
	ha	ha	ha	%
2009	7305	9147	−1842	−20.1
2016	8447	11496	−3049	−26.5

The substantial ‘underestimation’ of the classifier compared to the statistical data can be traced back to different methodological approaches. Whereas statistical data are field based, the remote-sensing classification approach provides pixel-based results. Thus, areas in the maize fields exhibiting spots of bare soil due to late sowing dates, erosion processes, damages by wild boars, and weak field emergence were (correctly) not classified as maize but were included in the official statistics as maize (Figure 3).

Moreover, due to the south to north gradient in vegetative development (see Supplementary Material Table S1), there is a quite short time slot suitable for classification based on optical satellite images. This weakness of the chosen approach could be overcome by using radar data, which makes image recording independent from cloud coverage. Moreover, a complete time series of maize cultivation sites would also allow answering the questions of mono-cultural growth of silage maize. However, for the years of this investigation, no suitable data, such as nowadays, e.g., provided by the Sentinel 2 platforms, were available.

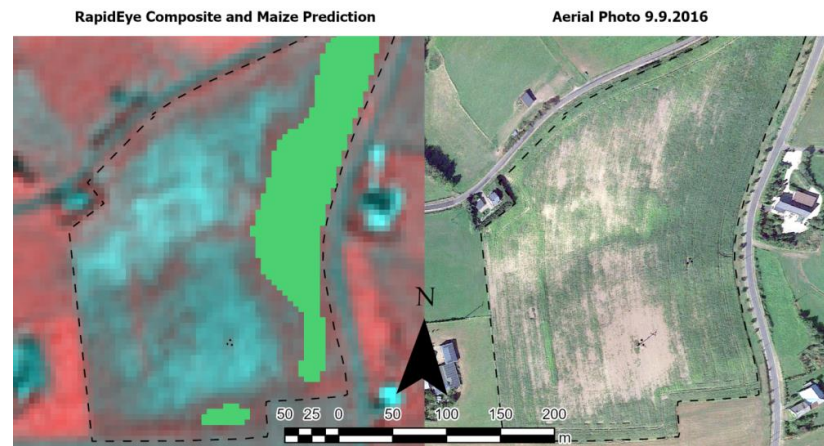


Figure 3. Visual clarification of different approaches of maize classification. Data included in the official statistics include the whole area of the maize field as shown by the dashed lines including large spots of bare soil as visible in the aerial photo. In contrast, the remote sensing-based classification approach only classifies pixel as ‘maize’ that are in fact maize-covered as shown by the prediction in green colour in the RapidEye composite.

3.2. Extent and Changes in Silage Maize Cultivation in the Study Area

In 2009 and 2016, 8.4 and 9.7% of the agricultural area were covered with maize, respectively. By the fact that more than 50% of the agricultural area was grassland and the size of arable land was increased from 36,610 ha to 42,439 ha in the same period (Figure 1), the share of silage maize on arable land amounted to about 20% in both years. However, large regional differences were observed (Figure 4). In 14 (2009) and 15 (2016) municipalities, silage maize was not cultivated. In the municipality with the highest share of silage maize, the cultivation area accounted for 29.9 (2009) and 34.2% (2016) of the agricultural area. Unfortunately, the share of arable land on the agricultural area is currently not available at municipal level, resulting in an inaccuracy in describing the relative proportion of silage maize cultivation in landscape.

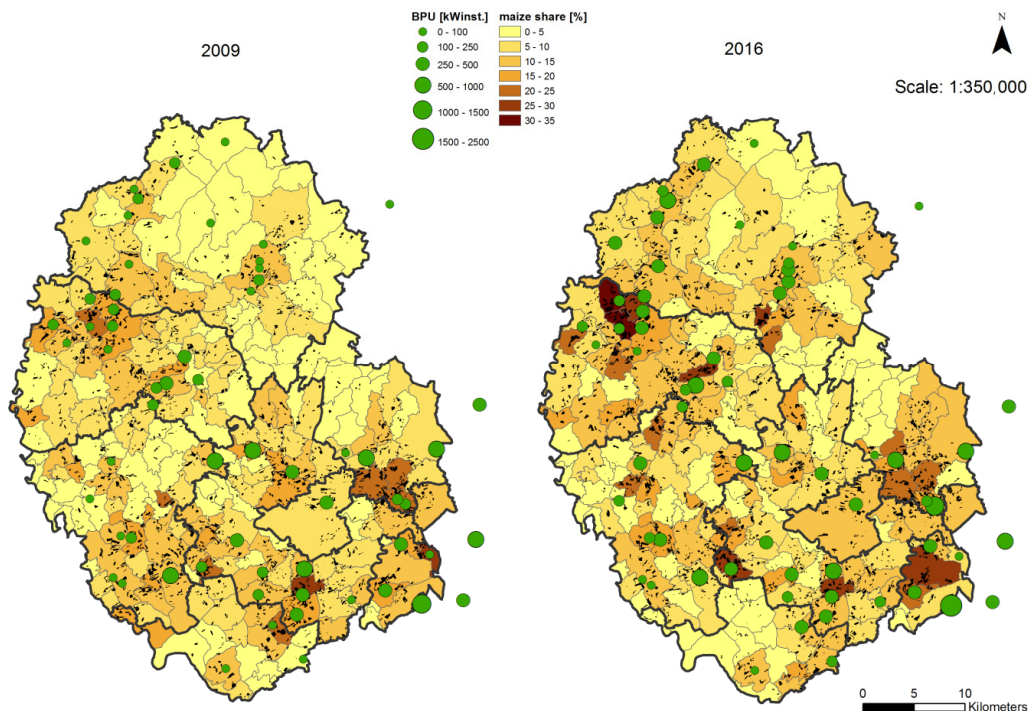


Figure 4. Representation of silage maize cultivation (black spots) and of the share of silage maize cultivation on agricultural land use based on the municipalities of the study area. Moreover, the location and size of the biogas producing units (BPU) is presented.

The changes in silage maize cultivation at municipal level apparently correlate with newly constructed or increased installed capacity of existing BPUs. Although, silage maize cultivated as feedstock for BPUs cannot be gathered separately from silage maize cultivated as fodder for ruminant production, there is evidence that the demands of BPUs are the drivers for expanded cultivation. The cattle stock in the study area steadily declines for around three decades (Figure 1). Moreover, regardless the final uses of the silage maize, the effects on soils are similar as there is no difference in the cultivation system. Figure 5 also implies that the feedstock sources for a certain BPU overlapped the borders of municipalities. Hot spots of increased silage maize cultivation and BPU capacity from 2009 to 2016 were detected in municipalities in the north-western part of the study region. These municipalities also showed the highest shares of silage maize on agricultural soil use in 2016 (Figure 4).

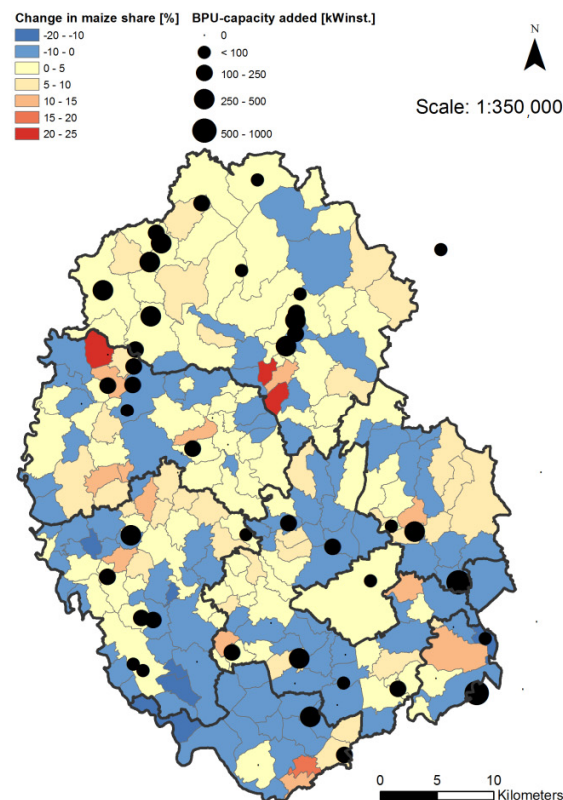


Figure 5. Representation of the changes in silage maize cultivation and the installed capacity of biogas producing units (BPU) from 2009 to 2016.

3.3. Maize Cultivation on Pedotopes Susceptible for Soil Compaction

Overall, 36.3% or 31,706 ha of the total agricultural area could be classified according to their susceptibility for soil compaction (Figure 6). Under the assumption that available data are representative for the whole study area, this would mean that 90.7, 7.0, and 2.3% show a low, medium, and high vulnerability for soil compaction, respectively (Table 5). Although the approach for classification of soils that are particularly vulnerable for compaction was suitable for an unbiased derivation of soil types from sequences of soil horizons given in the data of Germany's land appraisal, the final results were not satisfying at all. The dataset was incomplete, since numerous soil profile descriptions were not available in a digital form or do not exist (M. Goldschmitt, Landesamt für Geologie und Bergbau Rheinland-Pfalz, personal communication, 02.07.2015). Moreover, lots of site descriptions showed apparent mistakes; thus, a classification was also not possible for these sites.

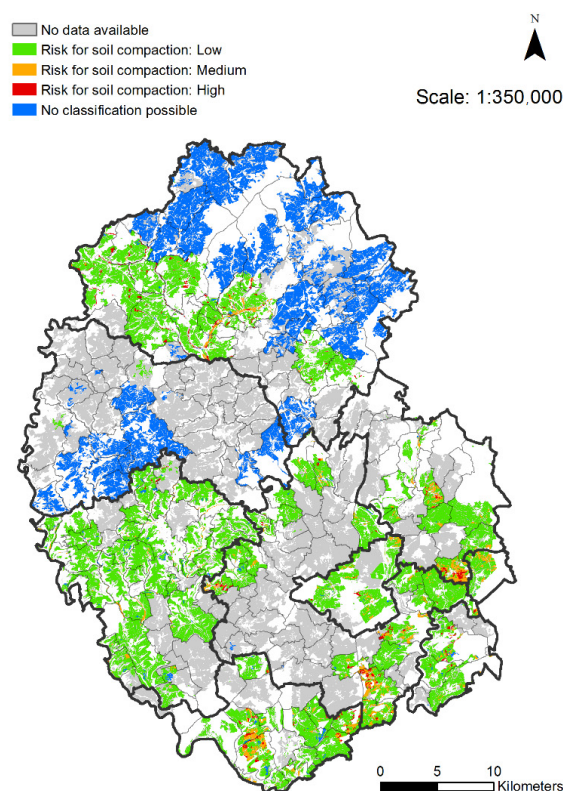


Figure 6. Representation of the susceptibility of the agricultural sites for soil compaction during harvesting action of silage maize. ‘Classification not possible’ refers to sites for which the soil profile descriptions showed apparent mistakes. When soil profile descriptions were not existing or not available in digital form, they were categorized as ‘No data available’. Areas shown in white colour are non-agricultural sites.

Table 5. Parameters specifying the quality of the data basis for the soil type classification approach. Assignment of the agricultural area as well as maize cultivation in 2009 and 2016 to the classified susceptibility for soil compaction.

	Agricultural Area		Maize 2009		Maize 2016		
	ha	%	ha	%	ha	%	
Total	87,422	100	7305	100	8447	100	
Classifiable	31,706	36.3	2867	39.2	3249	38.5	
Vulnerability for soil compaction	Low	28,758	90.7	2567	89.5	2997	92.2
	Medium	2226	7.0	252	8.8	195	6.0
	High	722	2.3	48	1.7	57	1.8

Based on the authors’ knowledge about soil type distribution in the study area, it appears that the soil profile descriptions from German land appraisal poorly represent the spatial heterogeneity of soil types. This becomes evident from large areas characterized as a single soil type and may result from the fact that the soil units in the framework of the German land appraisal should have a size of about one hectare (M. Beck, valuator of land appraisal in the Federal District of St. Wendel, personal communication, 18.10.2018). Likely, this particularly leads to an underestimation of Stagnosols, which show a patchy, small-scale distribution in low-mountain regions, particularly in dips, on planes, and at foots of slopes [35,36], which may not be well represented in the soil valuation units. Thirdly, the borders of the local authorities (thick lines in Figure 6) also mark breaking lines. It may be hypothesized that this indicates different pedological knowledge of the land

valuators. Generally, valuers of land appraisal in Germany are no experts in soil science and may thus overlook redoximorphic features indicating stagnant water in soils [32].

In contrast to other approaches that coupled soil physical and hydrological models to derive information about the trafficability of soils in the course of time [37], the approach used in this study used a single information base aiming to conclude for the potential susceptibility for compaction based on specific soil types associated with harvesting operations of silage maize. Thus, the amount of input data necessary to conclude for soil types is much lower compared for example to the approach of [38], who used pedotransfer functions and data about bulk density and the pre-compression stress in order to estimate the soil compaction hazard. Furthermore, sophisticated modeling approaches of the soils' carrying capacity at specific points of time were not meaningful in this case because of (i) the insufficient data basis, (ii) the large size of study area, and (iii) the impossibility to validate the modelled data. Moreover, such approaches would add a temporal dimension to the data analysis as soil water contents show a high temporal dynamics.

However, similar to the concept perused in this study, also the more sophisticated approach of [38] does not allow deriving time-resolved maps of the risk for soil compaction.

As a result of the fragmentary data basis (Section 3.3, Figure 6), less than 40 %, or 2867 (2009) and 3249 ha (2016), of silage maize cultivation could be overlapped with the map of soil compaction risk (Table 5). Thereof, 8.8 (2009) and 6.0% (2016) were cultivated on soils with a medium risk for compaction and slightly less than 2.0 % in both years on soils showing a high risk for compaction. Extrapolated to the whole study area, this would mean that approximately 500 to 600 ha of silage maize cultivation was done on soils that show a medium risk for soil compaction during silage maize harvesting. Another 150 to 160 ha of silage maize was grown on sites that are highly susceptible for compaction, both assuming that the available data are representative for the whole study area.

Due to the above mentioned deficiencies in raw data, these values should be regarded as a rough estimate. Furthermore, by extrapolating to the whole study area, the spatial explicit character of the study approach gets lost. Nonetheless, the presented example impressively shows the difficulties in conducting rather simple risk evaluations due to limitations in suitable and available input data. Although comprehensive soil maps exist, they were also finally based on the same basis of data and regionalized by geostatistical methods. Thus, subject to these conditions, more complex and virtually more precise methods, such as pedotransfer functions, are therefore currently not applicable in a landscape context.

To reduce the risk for soil compaction, a substitution from silage maize to perennial energy crops (PECs) can be suggested. In this aspect the benefits of PECs result from (i) earlier harvesting under dryer soil conditions and (ii) the permanent, intense routing system both enhancing the carrying capacity of the soil [39,40].

3.4. Natural Susceptibility of the Soils for Erosion and Threats to Soil Due to Maize Cultivation

The modeling of the natural susceptibility of the soils for erosion processes revealed a small-scale pattern typical for the conditions in a low mountain landscape with a mean E_{nat} value of $31.1 \text{ t ha}^{-1} \text{ a}^{-1}$ (Figure 7). A total of 20% of the agricultural sites were classified to have a low or very low susceptibility for soil erosion with natural erosion rates $<10 \text{ t ha}^{-1} \text{ a}^{-1}$ (Table 6). At the same time, nearly 50% of the agricultural area were classified to have a high to very high susceptibility for soil erosion ($E_{nat} > 25 \text{ t ha}^{-1} \text{ a}^{-1}$).

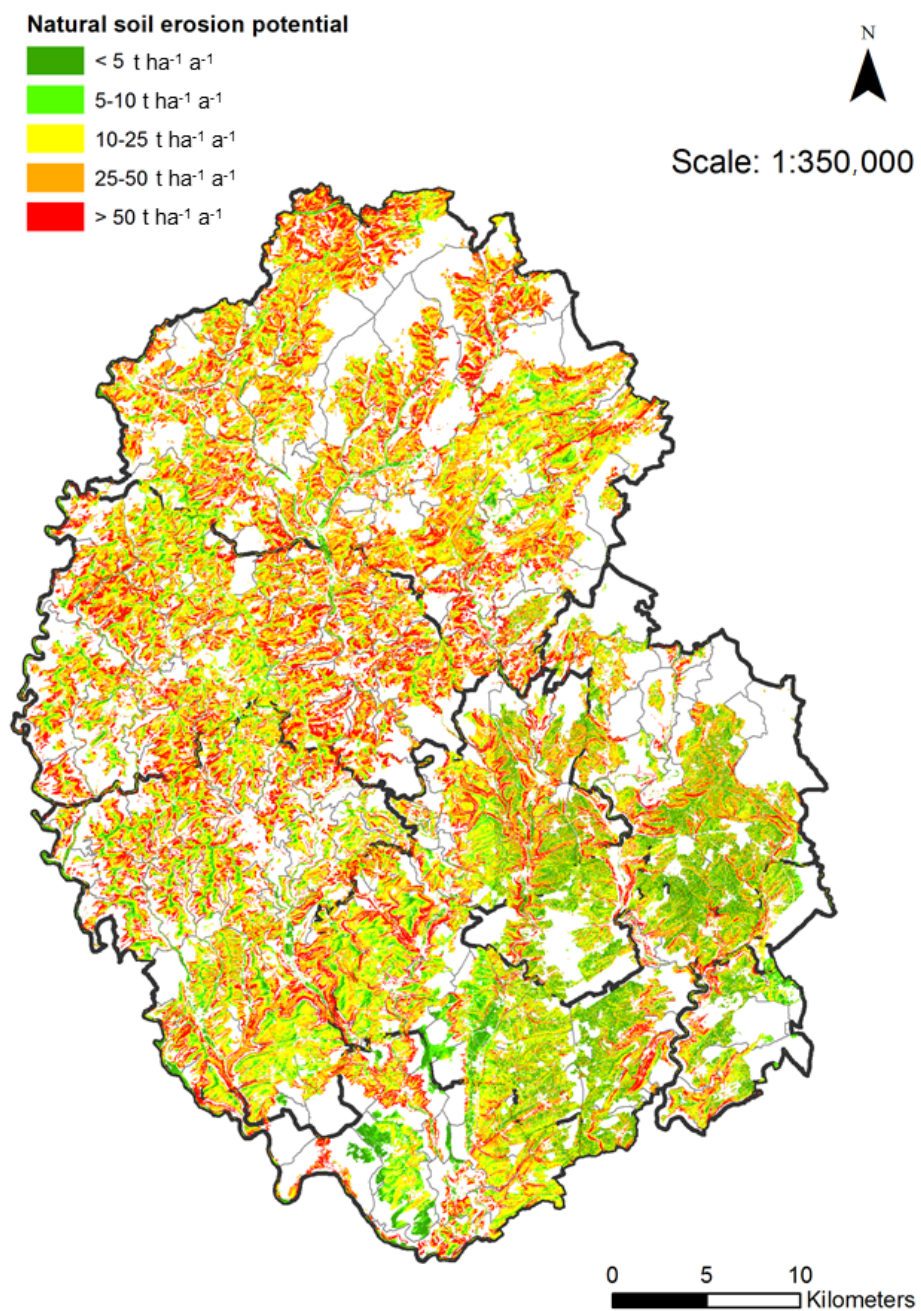


Figure 7. Map showing the calculated natural potential for soil erosion (E_{nat}) in the study area. Areas shown in white colour are non-agricultural sites and were thus excluded from erosion modeling.

Table 6. Assignment of the total agricultural area as well as maize and non-maize (all agricultural soil uses except maize) cultivation in 2009 and 2016 to the classified natural soil erosion potential (E_{nat}).

Erosion Potential	Agricultural Area		2009				2016			
			Maize		Non-Maize		Maize		Non-Maize	
	ha	%	ha	%	ha	%	ha	%	ha	%
Very low	8335	9.5	724	10.4	7611	9.5	791	9.7	7545	9.5
Low	9268	10.6	1034	14.8	8233	10.2	1147	14.1	8121	10.2
Medium	29,414	33.7	3045	43.6	26,369	32.8	3508	43.2	25,906	32.7
High	25,126	28.8	1846	26.5	23,280	29.0	2249	27.7	22,877	28.9
Very high	15,256	17.5	330	4.7	14,926	18.6	426	5.3	14830	18.7

The rainfall ('R') factor showed, similar to the topography ('S') factor, a distinct south to north gradient finally leading to a high natural soil erosion potential throughout the northern part of the study region. In contrast to that, the erodibility of the soils (K factor) in the southern part of the study region is considerably elevated due to higher silt contents of the soils. Nonetheless, in the southern part, the susceptibility for soil erosion is generally lower than in the northern part resulting from the more gentle slopes. For the arable land in Rhineland Palatinate, [41] calculated mean actual erosion rates (E_{nat} values multiplied by the cropping management factor C) of $11.2 \pm 22.9 \text{ t ha}^{-1} \text{ a}^{-1}$. Thus, the values calculated for the study region appear valid considering the low mountain character of the study region and the large standard deviation stated by [41].

In 2009 and 2016, more than 30% of the total silage maize cultivation was done on sites showing at least a high potential for soil erosion, whereby the area of silage maize cultivated on these sites increased from 2176 to 2675 ha. The mean E_{nat} value of fields cultivated with silage maize increased from 21.1 to $21.9 \text{ t ha}^{-1} \text{ a}^{-1}$. Thus, it can be concluded that the silage maize cultivation was distinctly expanded on sites that show high or very high erosion potential—sites that are subject to the cross compliance regulations of the European Union ($\text{CC}_{\text{water}1}$: $E_{\text{nat}} 15\text{--}27.5 \text{ t ha}^{-1} \text{ a}^{-1}$; $\text{CC}_{\text{water}2}$: $E_{\text{nat}} > 27.5 \text{ t ha}^{-1} \text{ a}^{-1}$) and national laws in order to 'prevent soil erosion' [42–44].

Finally, this indicates that the cultivation of silage maize is done largely ignoring the site conditions. On the one hand, this confirms the statement of [45] that "farmers clearly did not consider erosion in their management decisions like field size or selection of crops". On the other hand, it expresses the scarcity of suitable agricultural land. Political incentives for feedstock cultivation have made a crucial contribution to expand silage maize cultivation to inadequate sites thus raising external costs of bioenergy production. Although no data about the specific management practice are available, strategies to prevent soil erosion are to our experience no common practice in the study area. For example, undersown crops, minimum tillage methods, or changes in cultivated crops may potentially reduce soil erosion rates by factors between two and ten [33,46,47].

Even worse, against the background of progressing climate change, with increased frequency and intensity of heavy precipitation events, particularly in spring [48], when maize fields show mostly bare soil, the calculated values for soil erosion rates are likely no more than a conservative estimate. In particular, the erosivity of the rainfall seems to be a weak point in soil erosion modeling likely leading to a significant underestimation of the currently prevailing erosion rates. Recent research has shown that presently used rain erosivity factors significantly underestimate the conditions by (i) methodological reasons and (ii) resulting from climate changes. Firstly, state of the art methods (rain radar), have revealed that R factors are about 60% higher than those presently used [49], which were based on the analysis of ombrometers with a limited spatial data density [50]. Secondly, in the course of climate change, erosivity of the rainfall has significantly increased compared to data collection periods of [49] or [51] as a result of (i) higher change of thunderstorms, (ii) larger size of the drops, (iii) reduced wind speed, and, thus, (iv) larger amounts of precipitation per rain event [52]. Accordingly, [52] state that rain erosivity increases by a rate of 10% every 6 years.

Summarizing, cultivation of silage maize at sites that show a high susceptibility for soil erosion, as presented in Table 6, was underpinned, on one hand, by observing a huge number of maize fields that visibly showed signs of erosion in aerial photos (Figure 3) and on the other hand by the discrepancy of the maize cultivation area compared to statistical data by remote-sensing based classification approach (Table 5). Areas of bare soil, like areas of erosion, transport, and accumulation, were classified as non-maize pixels due to the soil signal (Figure 3).

4. Conclusions

This spatial study depicts an illustrative example in which way political measures, such as subsidies, may influence the agricultural land-use implying negative consequences

for soil health. The additional demand for feedstocks in the study area has led to land-use pressure and significant problems in sustaining soil health in the study region. The combination of remote sensing-based maize classification and target-specific analysis of the soils' vulnerability allowed for a spatially explicit estimation of the site-specific hazard potential. Unfortunately, the data quality for estimating the risk for soil compaction was insufficient to a large extent. Nonetheless, soil erosion seems to represent the more important threat to soil health. However, by the fact that eroded patches and areas with weak field emergence were not detected as maize by the classification, the results certainly present conservative estimates, particularly when considering the predicted impacts of climate change.

The chosen approach to identify the site-specific vulnerability for soil compaction and erosion presents a valuable tool for decision support, aiming for a strategically planned and thus more sustainable energy crop cultivation. It can be used to initiate countermeasures in order to meet the demands of both valuable feedstock production and soil protection, as well as to sensitize farmers for the long-term consequences of soil degradation. A further development of the presented concept may support farmers in their crop selection and management strategy, e.g., in the form of a smartphone app. However, the availability of comprehensive and small-scale valid soil data presents the bottleneck of the approach.

In the long term, sustaining or improving soil health is inevitable in order to maintain the production function of agricultural soils.

Supplementary Materials: The following are available online at <https://www.mdpi.com/2073-445X/10/2/128/s1>, Table S1: Characterization of the climatic gradient present in the study area on the basis of long-term mean monthly temperature and precipitation data (1981–2010) of three meteorological stations located in the southern, central, and northern part of the study area. Data derived from German Meteorological Service (2018). Figure S1: Flowchart explaining the steps and methods for the remote sensing based classification of maize fields acc. to [53]. Figure S2: Flowchart explaining the steps for classification of soil types based on site-specific sequences of soil horizons.

Author Contributions: Conceptualization, T.R. and M.G.; methodology, T.R. and M.G.; data analysis, visualization, and interpretation T.R.; writing—original draft preparation, T.R.; writing—review and editing, T.R.; supervision, C.E. and T.U.; project administration, C.E. and T.U. All authors have read and agreed to the published version of the manuscript.

Funding: This research received no external funding. Imagery was provided by Planet Labs, Inc. under the RapidEye Science Archive (RESA) program. Project ID: 00197.

Data Availability Statement: Data available on request due to restrictions.

Acknowledgments: Imagery was provided by Planet Labs, Inc. under the RapidEye Science Archive (RESA) program. Project ID: 00197. The publication was funded by the Open Access Fund of University of Trier and the German Research Foundation (DFG) within the Open Access Publishing funding program.

Conflicts of Interest: The authors declare no conflict of interest.

References

1. Braun, R.; Weiland, P.; Wellinger, A. Biogas from Energy Crop Digestion. IEA Bioenergy Task 37: Energy from Biogas and Landfill Gas. 2010. Available online: http://task37.ieabioenergy.com/files/daten-redaktion/download/energycrop_def_Low_Res.pdf (accessed on 12 September 2018).
2. Lupp, G.; Albrecht, J.; Darbi, M.; Bastian, O. Ecosystem services in energy crop production: A concept for regulatory measures in spatial planning? *J. Landsc. Ecol.* **2011**, *4*, 49–66. [CrossRef]
3. Erneuerbare-Energien-Gesetz (EEG), Gesetz für den Ausbau Erneuerbarer Energien vom 21. Juli 2014 (BGBl. I S. 1066, Berlin), das Durch Artikel 2 des Gesetzes vom 22. Dezember 2016 (BGBl. I S. 3106, Berlin) Geändert Worden Ist. Available online: https://www.gesetze-im-internet.de/eeg_2014/BJNR106610014.html (accessed on 14 September 2020).
4. Deutsches Biomasseforschungszentrum (DBFZ). *Anlagenbestand Biogas und Biomethan—Biogaserzeugung und-Nutzung in Deutschland*; Report Nr. 30; DBFZ: Leipzig, Germany, 2017.
5. Fachagentur Nachwachsende Rohstoffe (FNR). *Basisdaten Bioenergie Deutschland 2014. Festbrennstoffe, Biokraftstoffe, Biogas*; Bestell-Nr. 469; FNR: Gülzow-Prüzen, Germany, 2014.

6. Fachagentur Nachwachsende Rohstoffe (FNR). *Basisdaten Bioenergie Deutschland 2018. Festbrennstoffe, Biokraftstoffe, Biogas*; FNR: Gülzow-Prüzen, Germany, 2018. Available online: http://www.fnr.de/fileadmin/allgemein/pdf/broschueren/Basisdaten_Bioenergie_2018.pdf (accessed on 11 September 2018).
7. KTBL (Kuratorium für Technik und Bauwesen in der Landwirtschaft e.V.). *Energiepflanzen. Daten für die Planung des Energiepflanzenanbaus*, 2nd ed.; KTBL: Darmstadt, Germany, 2012.
8. Weiland, P. Biogas production: Current state and perspectives. *Appl. Microbiol. Biotechnol.* **2010**, *85*, 849–860. [[CrossRef](#)] [[PubMed](#)]
9. Adler, P.R.; Del Grosso, S.J.; Parton, W.J. Life-cycle assessment of the net greenhouse-gas flux for bioenergy cropping systems. *Ecol. Appl.* **2007**, *17*, 675–691. [[CrossRef](#)] [[PubMed](#)]
10. Blanco-Canqui, H. Energy crops and their implications on soil and environment. *Agron. J.* **2010**, *102*, 403–419. [[CrossRef](#)]
11. Herrmann, A. Biogas production from maize: Current state, challenges and prospects. 2. Agronomic and environmental aspects. *BioEnergy Resear.* **2013**, *6*, 372–387.
12. Immerzeel, D.J.; Verweij, P.A.; van der Hilst, F.; Faaij, A.P.C. Biodiversity impacts of bioenergy crop production: A state-of-the-art review. *Glob. Chang. Biol. Bioenergy* **2014**, *6*, 183–209. [[CrossRef](#)]
13. Statistisches Landesamt Rheinland-Pfalz (Statistical Office Rhineland-Palatinate). *Statistisches Jahrbuch 2017, Rheinland-Pfalz*; Statistisches Landesamt Rheinland-Pfalz: Sinzig, Germany, 2017.
14. DLR Mosel, Daten zum Silomaisanbau in der Region Trier und in Rheinland-Pfalz. 2018. Available online: <http://www.dlr-mosel.rlp.de/Internet/global/themen.nsf/d0e5087e9e1e8b79c1257abf0060c5df/b7c65bbd218ffd94c1257c1c004c2c99?OpenDocument> (accessed on 12 September 2018).
15. Statistisches Landesamt Rheinland-Pfalz (Statistical Office Rhineland-Palatinate). *Statistische Bände: Die Landwirtschaft mit Vergleichszahlen seit 1949*; Statistisches Landesamt Rheinland-Pfalz: Bad Ems, Germany, 1949; multiple years.
16. Von Francken-Welz, H.; Wenghoefer, V.; Hamilton, V. Biogasanlagen in Rheinland-Pfalz 2017. 5. Betriebserhebung Biogas. Dienstleistungszentrum Ländlicher Raum Eifel (publ.), Germany. 2017. Available online: [http://www.dlreifel.rlp.de/Internet/global/themen.nsf/3377acc1e3e31fb8c12579f000322e61/c661a290b8aef10ec12581f300343635/\\$FILE/Biogaserhebung2017_final.pdf](http://www.dlreifel.rlp.de/Internet/global/themen.nsf/3377acc1e3e31fb8c12579f000322e61/c661a290b8aef10ec12581f300343635/$FILE/Biogaserhebung2017_final.pdf) (accessed on 18 July 2018).
17. Landesamt für Vermessung und Geobasisinformation Rheinland-Pfalz (LVerGeo). *Digital Elevation Model with a Grid Width of 5 m (DEM5)*; Landesamt für Vermessung und Geobasisinformation Rheinland-Pfalz (LVerGeo): Koblenz, Germany, 2018.
18. Steingötter, K. *Geologie von Rheinland-Pfalz. Landesamt für Geologie und Bergbau Rheinland-Pfalz (Hrsg.)*; E. Schweizerbart'sche Verlagsbuchhandlung (Nägele u. Obermiller): Stuttgart, Germany, 2005.
19. German Meteorological Service, Climate Data Center. Available online: ftp://ftp-cdc.dwd.de/pub/CDC/observations_germany/climate/multi_annual/mean_81-10/ (accessed on 20 July 2018).
20. Landesamt für Geologie und Bergbau Rheinland-Pfalz (LGB-RLP) (State Office for Geology and Mining Rhineland-Palatinate): Geologische Übersichtskarte von Rheinland-Pfalz: Online Karte GÜK 300. 2018. Available online: <http://www.lgbrlp.de/karten-und-produkte/online-karten/online-karte-guek-300.html> (accessed on 18 July 2018).
21. Landesamt für Geologie und Bergbau Rheinland-Pfalz (LGB-RLP) (State Office for Geology and Mining Rhineland-Palatinate) Bodenflächendaten 1:200,000. 2018. Available online: <http://www.lgb-rlp.de/karten-und-produkte/wms-dienste.html> (accessed on 18 July 2018).
22. Wagner, W.; Negendank, J.F.W.; Fuchs, G.; Mittmeyer, H.G. *Geologische Übersichtskarte: Rheinisches Schiefergebirge SW-Teil 1:100,000*; Geologisches Landesamt Rheinland-Pfalz, Ed.; Geologisches Landesamt Rheinland-Pfalz: Mainz, Germany, 1983.
23. Tanré, D.; Deroo, C.; Duhaut, P.; Herman, M.; Morcrette, J.J.; Perbos, J.; Deschamps, P.Y. Technical note. Description of a computer code to simulate the satellite signal in the solar spectrum: The 5S code. *Int. J. Remote Sens.* **1990**, *11*, 659–668. [[CrossRef](#)]
24. Hill, J.; Sturm, B. Radiometric correction of multitemporal Thematic Mapper data for use in agricultural land-cover classification and vegetation monitoring. *Int. J. Remote Sens.* **1991**, *12*, 1471–1491. [[CrossRef](#)]
25. Hill, J.; Mehl, W.; Radeloff, V. Improved forest mapping by combining corrections of atmospheric and topographic effects in Landsat TM imagery. In *Sensors and Environmental Applications of Remote Sensing, Proceedings of the 14th EARSeL Symposium, Göteborg, Sweden, 6–8 June 1994*; Askne, J., Ed.; Chalmers University of Technology: Göteborg, Sweden, 1995; pp. 143–151.
26. R Core Team. *R: A Language and Environment for Statistical Computing*; R Foundation for Statistical Computing: Vienna, Austria, 2016. Available online: <https://www.R-project.org/> (accessed on 19 January 2021).
27. Wright, M.N.; Ziegler, A. Ranger: A fast implementation of random forests for high dimensional data in C++ and R. *J. Stat. Softw.* **2017**, *77*, 1–17. [[CrossRef](#)]
28. Breiman, L. Random Forests. *Mach. Learn.* **2001**, *45*, 5–32. [[CrossRef](#)]
29. Belgiu, M.; Draăgut, L. Random forest in remote sensing: A review of applications and future directions. *ISPRS J. Photogramm. Remote Sens.* **2016**, *114*, 24–31. [[CrossRef](#)]
30. Ad-hoc-AG Boden. *Bodenkundliche Kartieranleitung*, 5th ed.; E. Schweizerbart'sche Verlagsbuchhandlung: Stuttgart, Germany, 2005.
31. Food and Agriculture Organization of the United Nations (FAO). *Guidelines for Soil Description*, 4th ed.; FAO: Rome, Italy, 2006.
32. Bodenschätzungsgesetz (BodSchätzG), Gesetz zur Schätzung des landwirtschaftlichen Kulturbodens vom 20. Dezember 2007 (Bundesgesetzblatt I S. 3150, 3176, Berlin), das durch Artikel 232 der Verordnung vom 31. August 2015 (Bundesgesetzblatt I S. 1474, Berlin) Geändert Worden ist. Available online: http://www.gesetze-im-internet.de/bodsch_tzg_2008/BodSchätzG.pdf (accessed on 14 September 2020).

33. Deutsches Institut für Normung (DIN). 19708:2017-08: *Soil Quality: Predicting Soil Erosion by Water by Means of the USLE (Bodenbeschaffenheit: Ermittlung der Erosionsgefährdung von Böden Durch Wasser Mithilfe der ABAG)*; Beuth-Verlag: Berlin, Germany, 2017.
34. Wischmeier, W.; Smith, D. *Predicting Rainfall Erosion Losses: A Guide to Conservation Planning*; Agriculture Handbook No. 537; U.S. Department of Agriculture: Hyattsville, MD, USA, 1978.
35. Blume, H.-P.; Brümmer, G.W.; Fleige, H.; Horn, R.; Kandeler, E.; Kögel-Knabner, I.; Kretzschmar, R.; Stahr, K.; Wilke, B.-M. *Scheffer/Schachtschabel. Soil Science*; Springer: Berlin/Heidelberg, Germany, 2016.
36. Zech, W.; Schad, P.; Hintermaier-Erhard, G. *Böden der Welt. Ein Bildatlas*, 2nd ed.; Springer Spektrum: Berlin/Heidelberg, Germany, 2014.
37. Kuhwald, M.; Dörrhöfer, K.; Oppelt, N.; Duttmann, R. Spatially explicit soil compaction risk assessment of arable soils at regional scale: The SaSciA-Model. *Sustainability* **2018**, *10*, 1618. [CrossRef]
38. Lebert, M. Entwicklung eines Prüfkonzeptes zur Erfassung der tatsächlichen Verdichtungsgefährdung landwirtschaftlich genutzter Böden. UBA-Texte 51/2010, Förderkennzeichen: 370771202. Available online: <https://www.umweltbundesamt.de/sites/default/files/medien/461/publikationen/4027.pdf> (accessed on 1 April 2019).
39. Ruf, T.; Audu, V.; Holzhauser, K.; Emmerling, C. Bioenergy from periodically waterlogged cropland in Europe: A first assessment of the potential of five perennial energy crops to provide biomass and their interactions with soil. *Agronomy* **2019**, *9*, 374. [CrossRef]
40. Schoo, B.; Schroetter, S.; Kage, H.; Schittenhelm, S. Root traits of cup plant, maize and lucerne grass grown under different soil and soil moisture conditions. *J. Agron. Crop Sci.* **2017**, *203*, 345–359.
41. Saggau, P.; Bug, J.; Gocht, A.; Kruse, K. Aktuelle Bodenerosionsgefährdung durch Wind und Wasser in Deutschland. *Bodenschutz* **2017**, *22*, 120–125.
42. European Union. *EU Regulation No 1306/2013, Regulation of the European Parliament and of the Council of 17 December 2013 on the Financing, Management and Monitoring of the Common Agricultural Policy and Repealing Council Regulations (EEC) No 352/78, (EC) No 165/94, (EC) No 2799/98, (EC) No 814/2000, (EC) No 1290/2005 and (EC) No 485/2008*; EU: Brussels, Belgium, 2013.
43. AgrarZahlVerpflG Gesetz zur Regelung der Einhaltung von Anforderungen und Standards im Rahmen Unionsrechtlicher Vorschriften über Agrarzahlungen. Agrarzahlungen-Verpflichtungengesetz vom 2. Dezember 2014 (Bundesgesetzblatt I S. 1928, Berlin). Available online: <https://www.gesetze-im-internet.de/agrarzahlverpflg/AgrarZahlVerpflG.pdf> (accessed on 14 September 2020).
44. AgrarZahlVerpflV Verordnung über die Einhaltung von Grundanforderungen und Standards im Rahmen Unionsrechtlicher Vorschriften über Agrarzahlungen. Agrarzahlungen-Verpflichtungenverordnung vom 17. Dezember 2014 (BAnz AT 23.12.2014 V1, Berlin), die zuletzt durch Artikel 2 der Verordnung vom 27. September 2018 (BAnz AT 28.09.2018 V1, Berlin) geändert worden ist. Available online: <https://www.gesetze-im-internet.de/agrarzahlverpflv/AgrarZahlVerpflV.pdf> (accessed on 14 September 2020).
45. Auerswald, K.; Fischer, F.K.; Kistler, M.; Treisch, M.; Maier, H.; Brandhuber, R. Behavior of farmers in regard to erosion by water as reflected by their farming practices. *Sci. Total Environ.* **2018**, *613–614*, 1–9. [CrossRef]
46. Panagos, P.; Borrelli, P.; Meusburger, K.; Alewell, C.; Lugato, E.; Montanarella, L. Estimating the soil erosion cover-management factor at the European scale. *Land Use Policy* **2015**, *48*, 38–50. [CrossRef]
47. Schwertmann, U.; Vogl, W.; Kainz, M. *Bodenerosion Durch Wasser. Vorhersage des Abtrags und Bewertung von Gegenmaßnahmen*; Verlag Eugen Ulmer: Stuttgart, Germany, 1987.
48. European Environmental Agency (EEA). *Climate Change, Impacts and Vulnerability in Europe 2016: An Indicator-Based Report (EEA Report No 1/2017)*; European Environment Agency: Copenhagen, Denmark, 2017.
49. Sauerborn, P. Die Erosivität der Niederschläge in Deutschland—Ein Beitrag zur quantitativen Prognose der Bodenerosion durch Wasser in Mitteleuropa. In *Bonner Bodenkundliche Abhandlungen*; Band 13; Universität Bonn: Bonn, Germany, 1994.
50. Auerswald, K.; Fischer, F.K.; Winterrath, T.; Brandhuber, R. Rain erosivity map for Germany derived from contiguous radar rain data. *Hydrol. Earth Syst. Sci.* **2019**, *23*, 1819–1832. [CrossRef]
51. Rogler, H.; Schwertmann, U. Erosivität der Niederschläge und Isoerodentkarte Bayerns. *Z. Kult. Flurberein.* **1981**, *22*, 99–112.
52. Auerswald, K.; Fischer, F.; Winterrath, T.; Elhaus, D.; Maier, H.; Brandhuber, R. Klimabedingte Veränderung der Regenerosivität seit 1960 und Konsequenzen für Bodenabtragsschätzungen. In *Bodenschutz, Ergänzbare Handbuch der Maßnahmen und Empfehlungen für Schutz, Pflege und Sanierung von Böden, Landschaft und Grundwasser (Loseblattsammlung)*; Bachmann, G., König, W., Utermann, J., Eds.; Erich Schmidt Verlag: Berlin, Germany, 2019.
53. Gilcher, M.; Ruf, T.; Emmerling, C.; Udelhoven, T. Remote sensing based binary classification of maize. Dealing with residual autocorrelation in sparse sample situations. *Remote Sens.* **2019**, *11*, 2172. [CrossRef]